Symmetry breaking and dynamical independence in a multimode laser

E. A. Viktorov
Institute for Laser Physics, 199034 St. Petersburg, Russia

A. G. Vladimirov
Physics Faculty, St. Petersburg State University, 198904 St. Petersburg, Russia

Paul Mandel
Optique Nonlinéaire Théorique, Université Libre de Bruxelles, Campus Plaine Code Postale 231, B-1050 Bruxelles, Belgium
(Received 5 November 1999; revised manuscript received 18 May 2000)

Multimode lasers display various behaviors caused by the asymmetry between the modes belonging to orthogonal polarizations. We discuss dynamical independence, clustering, and grouping in a solid state laser with intracavity second harmonic generation, and show that these effects result from unstable cycles lying within their invariant planes. These invariant planes are dynamically independent. The sequential or random itinerancy of limit unstable cycles lying within the invariant planes explains most of the effects caused by asymmetry.

PACS number(s): 05.45.−a, 05.40.−a, 42.65.Pc

I. INTRODUCTION

In a recent publication [1], we have analyzed dynamical properties of a multimode laser with intracavity second harmonic generation with all N modes oscillating with the same polarization of the electric field. The symmetry of the model results in an $(N-1)$-fold degenerate Hopf bifurcation of the N-mode steady state, which leads to dynamics on $(N-1)!$ periodic or quasiperiodic attractors, characterized by antiphased oscillations, i.e., equally phase-shifted oscillations with the same amplitude [2]. Spontaneous symmetry breaking can also occur and produces new solutions characterized by different oscillation amplitudes.

In this paper we consider second harmonic generation in a Fabry-Perot cavity containing birefringent elements, such as the neodymium-doped yttrium aluminum garnet (Nd:YAG) laser with intracavity potassium titanyl phosphate (KTP). The presence of birefringent elements destroys the symmetry between the two polarizations and each longitudinal mode of the multimode cavity splits into a pair of orthogonally polarized electric field components propagating at different velocities. A model has been developed over the years to describe the Nd:YAG/KTP laser [3] to account for the polarization properties [4,5]. In the rate equation limit, the modal intensities I_m and nonlinear gains G_m satisfy the evolution equations

$$\eta \frac{dI_m}{dt} = I_m\left(G_m - \alpha + \varepsilon g I_m - 2\varepsilon \sum_r^N \mu_{mr} I_r \right) + \sigma_m , \quad (1)$$

$$\frac{dG_m}{dt} = \gamma - G_m\left(1 + (1-\beta) I_m + \beta \sum_r^N I_r \right), \quad (2)$$

where $\eta = \tau_c / \tau_f$ is the ratio of the cavity round trip time τ_c and the fluorescence lifetime τ_f. The cavity loss parameter is α and the linear gain of mode m is γ. The mode index m varies from 1 to N, the number of oscillating modes. A measure of the conversion efficiency of the fundamental frequency intensity into the frequency-doubled intensity is ε, and β is the cross saturation parameter. σ_m represents an injected field. If the linearly polarized modes m and r have the same polarization $\mu_{mr} = g$, where $0 \leqslant g \leqslant 1$ is a geometrical factor whose value depends crucially on the angle between the fast axes of the active and doubling crystals as well as the phase delays due to their birefringence. Otherwise $\mu_{mr} = 1 - g$. Experimentally, the relevant domain of parameters is $\varepsilon, \eta \ll 1$ and $\alpha, \beta, \gamma, \varepsilon / \eta = O(1)$.

The steady-state solutions of Eqs. (1) and (2) and conditions for Hopf bifurcation were first analyzed in [6]. Another dynamical scenario and mode hopping between different states are described in [7]. It was shown in that reference that the mode hopping in a frequency-doubled laser is similar to the antiphase self-modulation regime in a bidirectional class B laser and arises after a global bifurcation [8].

Birefringent elements have two orthogonal optical axes, the ordinary and extraordinary axes, with different refractive indices and therefore different speeds of light along these two directions. This breaks the symmetry among the cavity lasing modes and induces in the laser a spatial asymmetry, which can lead to a situation where the dynamics of modes with orthogonal polarizations can be nonreciprocal: modes in one polarization influence modes in the other polarization but not the converse. It was reported in [9] that, when two modes oscillate in one polarization and a single mode oscillates in the orthogonal polarization, the two modes can display chaos while the orthogonal mode remains apparently periodic despite global coupling. Small amplitude noise added to the system does not affect this dynamical independence. For $N > 3$, the signature of nonreciprocal independence has been found in several situations such as the formation of clustered and grouped states. In the N-mode clustered regime, $N-M$ modes oscillate in phase and M modes antiphase; in general, the in-phase modes have the same polarization [10]. Grouped states display modal intensities with different oscillation periods (usually with rational

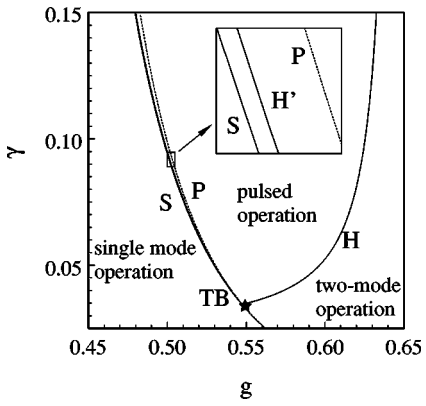

FIG. 1. Laser operating in two modes with orthogonal polarizations. Bifurcation loci for the steady-state solutions of Eqs. (1) and (2) with $\eta=0.002$, $\varepsilon=0.05$, $\alpha=0.02$, $\beta=0.292$. The boundary H indicates a Hopf bifurcation from the symmetric two-mode steady state $I_1=I_2$. The boundary S is the stability boundary of the single-mode solutions, which are stable below this boundary. The boundary P is above the boundary S and corresponds to a pitchfork bifurcation of the two-mode regime. Asymmetric two-mode steady states exist between S and P and exhibit a Hopf bifurcation at the curve H'. TB is a codimension-2 point resulting from the interaction between the steady state and the Hopf bifurcation.

ratios) in different polarizations and can exhibit a self-induced switching among grouped patterns [11].

The present study is motivated by the fact that birefringent-induced asymmetric oscillations can be induced by external modulation at suitable frequencies [12] and exploited in cryptography [13]. This paper is organized as follows. In Sec. II, we analyze the case of two modes with different polarizations, which is essential for the understanding of the dynamical effects caused by the asymmetry. In Sec. III, we investigate the three-mode case and the effect of dynamical independence. We then consider the noise influence in Sec. IV and conclude in Sec. V with a discussion of the clustered states.

II. TWO-MODE LASER MODEL: GLOBAL BIFURCATION

Consider the simplest case of a laser operating in two orthogonally polarized modes ($N=2$). The bifurcation diagram in the (g,γ) plane is shown in Fig. 1 in the absence of injected signal ($\sigma_{1,2}=0$). The steady-state solution, characterized by equal modal intensities ($I_1=I_2$), loses its stability on the boundary H, which indicates a Hopf bifurcation, leading to an antiphased periodic regime. The boundary P indicates a pitchfork bifurcation of the $I_1=I_2$ steady state, which leads to a pair of unstable steady states with unequal modal intensities $I_1>I_2$ ($I_1<I_2$). The asymmetry in the amplitudes of the modal intensities, which can be characterized by the quantity $|I_1-I_2|$, increases with the distance from the pitchfork bifurcation, and finally the asymmetric solution $I_1>I_2$ ($I_1<I_2$) collides with the single-mode steady state $I_1>0$, $I_2=0$ ($I_2>0, I_1=0$) at the boundary S. The single-mode steady states are stable to the left of the curve S. The boundaries S and P are very close to each other in Fig. 1 as can be seen in the inset. Asymmetric two-mode steady states with $I_1>I_2$ and $I_1<I_2$ exist in the narrow strip between S and P. They are stable below the line H' and unstable above this line. The point TB on P is a $\mathbf{Z}_2$-symmetric Takens-Bogdanov codimension-2 bifurcation for the $I_1=I_2$ steady-state solution. It is the limit point of the curve H. At this point the Jacobian matrix of Eqs. (1) and (2) has a double zero eigenvalue. According to local analysis of the dynamics near the Takens-Bogdanov bifurcation [14], there can be two different bifurcation scenarios of the breakup of the antiphase periodic regime that bifurcates at the curve H. The result depends on the parameters of the normal form equations. The first scenario is associated with a global bifurcation that forms a pair of heteroclinic orbits connecting the asymmetric two-mode steady states $I_1>I_2$ and $I_1<I_2$. This case was already described in [7]. Another scenario occurs for the parameter values of Fig. 1. We find numerically that there is a global bifurcation responsible for the breakup of the antiphase periodic regime. The bifurcation takes place between the curves S and H' where the asymmetric steady states are stable and, hence, there exists a very narrow bistability domain between the antiphase periodic and steady-state regimes. We show the type of global bifurcation from a normal form analysis [14]. According to this analysis performed in the vicinity of the TB point, a pair of unstable asymmetric periodic solutions bifurcates subcritically at H' and then glue into a single unstable symmetric limit cycle. The gluing occurs via a global bifurcation with a pair of orbits homoclinic to the $I_1=I_2$ steady state. The unstable symmetric cycle collides with the stable antiphase periodic solution bifurcating at the curve H and both cycles disappear. This global saddle-node bifurcation is responsible for the breakup of the antiphase periodic regime that appears via a Hopf bifurcation at the curve H.

We want to stress the similarity between the two different bifurcation scenarios, which is a direct consequence of the parameter domain relevant to experiments, $\eta,\varepsilon\ll 1$. The asymmetric steady states exist in a very narrow domain and global bifurcations leading to a breakup of the antiphase periodic regime occur very close to the boundary S. Therefore, when the system is close to the breakup of the antiphase periodic regime, the phase trajectory goes into very close proximity of the single-mode steady states, and the periodic solution looks like a hopping between two single-mode states, similar to that described in [7]. The phase trajectory and steady states are shown in Fig. 2.

If $N>2$, the two-mode antiphase cycles persist in the invariant planes characterized by only two nonzero modal intensities, and are stable within these planes. Although these cycles can be unstable with respect to perturbations transverse to invariant planes, they give a key to understanding the dynamical behaviors resulting from the asymmetry between orthogonal polarizations.

III. THREE-MODE LASER MODEL: DYNAMICAL INDEPENDENCE

Let us now move to the case of a laser operating in three linearly polarized modes. The polarizations can be either parallel or orthogonal. The asymmetry between modes in Eqs. (1) and (2) is described by the fact that $g\neq 0.5$. Let the modes 1 and 3 be in the same polarization state whereas the mode 2 is in the orthogonal polarization. Bifurcation loci for Eqs. (1) and (2) with $N=3$ and $\sigma_{1,2,3}=0$ are shown in Fig. 3.

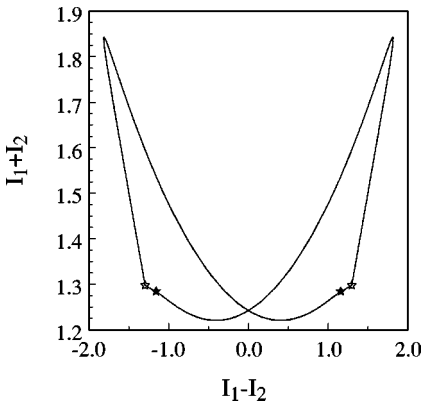

FIG. 2. Periodic antiphase regime in a laser operating in two modes with orthogonal polarizations. Filled (empty) stars indicate the location of the single-mode (asymmetric two-mode) steady states. The phase trajectory visits a very close proximity of the single-mode steady states, as is known to occur close to a heteroclinic bifurcation point. However, local analysis in the vicinity of the Takens-Bogdanov point predicts another type of global bifurcation. $g=0.49, \gamma=0.119$. Other parameters are as in Fig. 1.

The parameters remain the same as in the previous section. The boundaries P_{101} and H_{101} (P_{110} and H_{110}) in Fig. 3 are the loci of the pitchfork and Hopf bifurcations for the two-mode steady-state solution $I_1=I_3$, $I_2=0$ ($I_1=I_2$, $I_3=0$ and $I_2=I_3$, $I_1=0$). The single-mode solutions are stable below the steady-state bifurcation loci S_{100} and S_{010}. They become unstable on increasing the pump parameter γ and mode hopping appears, displaying an antiphased dynamics. Note that the bifurcations at the curves P_{110}, H_{110}, and S_{010} take place

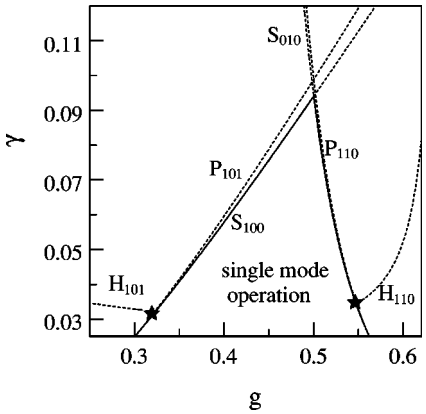

FIG. 3. Bifurcation loci Bifurcation loci for the steady-state solutions of Eqs. (1)–(2) for a three-mode laser. Modes 1 and 3 have the same polarization, mode 2 is in the orthogonal polarization. Parameters are the same as in Fig. 1. The boundary H_{101} indicates a Hopf bifurcation of the two-mode steady state with equal intensities in the same polarization $I_1=I_3>0$ and $I_2=0$ belonging to the invariant hyperplane Σ_{101}. The boundary P_{101} is above the boundary S_{100} and corresponds to a pitchfork bifurcation of this steady state. The single-mode steady-state solutions are stable below the boundaries S_{100} and S_{010}. The boundaries H_{110} and P_{110} indicate Hopf and pitchfork bifurcations of the two-mode steady-state solutions $I_1=I_2>0$, $I_3=0$ and $I_3=I_2>0$, $I_1=0$, which belong to the invariant hyperplanes Σ_{110} and Σ_{011}, respectively. Asterisks show the positions of codimension-2 points resulting from the interaction between steady-state and Hopf bifurcations.

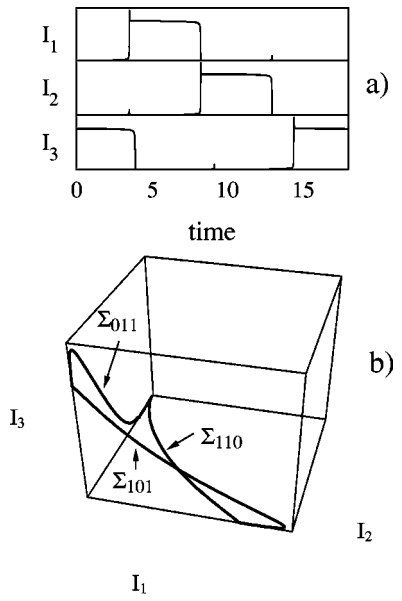

FIG. 4. Three-mode laser with all modal parameters identical, $g=0.5$, $\gamma=0.095$, $\sigma_{1,2,3}=0$. Other parameters are the same as for Fig. 3. (a) Intensity time traces indicate regular antiphase mode hopping; (b) three-dimensional (3D) phase portrait as a sequential itinerancy in the hyperplanes $\Sigma_{011}\rightarrow\Sigma_{101}\rightarrow\Sigma_{110}\rightarrow\Sigma_{011}$.

in invariant hyperplanes where only two modes with orthogonal polarizations have nonzero intensities. Therefore, these curves coincide with the curves P, H, and S in Fig. 1.

If the parameter g is small enough, the antiphased oscillations involve only two modes belonging to the same polarization, whereas the third mode with orthogonal polarization has zero intensity.

If $g=0.5$, all modes are equivalent in Eqs. (1) and (2) and oscillate with nonzero intensities. The temporal dynamics is a periodic hopping featuring antiphase dynamics as shown in Fig. 4(a): all modes oscillate identically but with a $2\pi/3$ phase shift between consecutive modes. The phase portrait of the antiphase three-mode limit cycle is presented in Fig. 4(b). The limit cycle consists of three segments, each lying near an invariant hyperplane characterized by only two nonzero modal intensities. The invariant hyperplanes Σ_{011}, Σ_{101}, and Σ_{110} are defined by $I_1=0$, $I_2=0$, and $I_3=0$, respectively. There are two sequences of hyperplane alternations corresponding to the two possible stable antiphase solutions: $\Sigma_{011}\rightarrow\Sigma_{101}\rightarrow\Sigma_{110}\rightarrow\Sigma_{011}$ and $\Sigma_{011}\rightarrow\Sigma_{110}\rightarrow\Sigma_{101}\rightarrow\Sigma_{011}$.

It is a trivial consequence of the symmetry between the modes for $g=0.5$ that each invariant hyperplane contains a limit cycle similar to the limit cycle responsible for the antiphase mode hopping in a two-mode laser, which was discussed in the previous section. Though this limit cycle is stable in its hyperplane, it can be unstable with respect to perturbations of the third mode, which has zero intensity. The cycles in the hyperplanes appear via Hopf bifurcations and disappear via global bifurcations that take place simultaneously for $g=0.5$.

If $g\neq0.5$ the modes are no longer equivalent. The symmetry of the model is broken for modes operating in orthogonal polarizations. The asymmetry introduced by $g\neq0.5$ splits the breakup boundaries for the antiphase periodic solutions lying in different hyperplanes. The breakup bound-

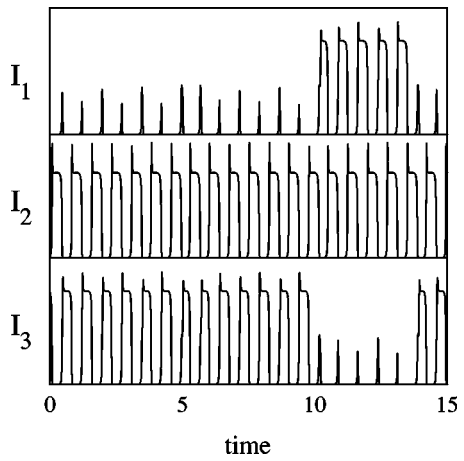

FIG. 5. Modal intensity time traces displaying dynamical independence. $g=0.5161$, $\gamma=0.095$. Other parameters are as in Fig. 4.

ary that destroys the two-mode unstable limit cycle in the hyperplane Σ_{101} occurs between the boundaries P_{101} and S_{100}. Another bifurcation takes place between the boundaries P_{110} and S_{010}. It is responsible for the breakup of the two-mode unstable limit cycles in the hyperplanes Σ_{011} and Σ_{110}.

If $g=0.5$, the laser equations (1) and (2) with all modes identical have another set of three invariant planes defined by $\{I_1=I_2, G_1=G_2\}$, $\{I_1=I_3, G_1=G_3\}$, and $\{I_2=I_3, G_2=G_3\}$. We denote these planes as Σ_{++1}, Σ_{+1+}, and Σ_{1++}, respectively. The asymmetry generated by $g\neq 0.5$ obviously destroys the invariant planes Σ_{++1} and Σ_{1++}, whereas the invariant plane Σ_{+1+}, for which the two modes with identical polarization have equal intensities ($I_1=I_3$), is preserved. The plane Σ_{+1+} contains an unstable cycle, important for our analysis. This cycle appears from a global bifurcation near the boundary S_{010} and is stable in Σ_{+1+}, but unstable with respect to transverse directions.

As mentioned above, if $g>0.5$ is large enough, the unstable limit cycle in Σ_{101} disappears after a collision with another periodic solution. The bifurcation sequence, including this bifurcation, produces significant qualitative changes in the antiphase motion shown in Fig. 4 for $g=0.5$. The motion near the invariant hyperplanes Σ_{011} and Σ_{110} remains and the two unstable limit cycles in these hyperplanes are still the destination for the phase trajectory, as shown in Figs. 5 and 6. However, the cycle in Σ_{101} no longer exists, and what is observed are jumps to and from the unstable limit cycle in Σ_{+1+}, as shown in Figs. 6–8. This cycle is characterized by the in-phase oscillations of modes in each polarization and out-of-phase oscillations between the two polarizations. Therefore, the two asymmetric attractors form a symmetric attractor by a ''gluing'' process in the invariant plane Σ_{+1+} [16].

Since the jumps to Σ_{+1+} take place either near to Σ_{101} where the orthogonally polarized mode I_2 has zero intensity or very close to the stable manifold of the cycle in Σ_{+1+}, they do not much affect the dynamics of that orthogonal mode, which appears periodic, whereas the two other modes display chaos caused by the jumps (see Fig. 5). This is the mechanism underlying dynamical independence [9]. The chaotic motion and jumps between the unstable cycles are illustrated also in Fig. 8. The phase trajectory spends almost

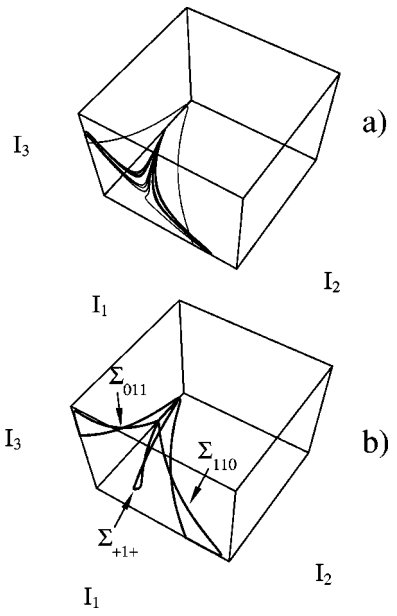

FIG. 6. (a) 3D phase portrait of the dynamical independence regime shown in Fig. 5. The phase trajectory exhibits random itinerancy between the limit cycles in the invariant planes Σ_{011}, Σ_{110}, and Σ_{+1+}. (b) Unstable limit cycles lying in the planes Σ_{011}, Σ_{110}, and Σ_{+1+}.

all its time in the vicinity of the three unstable cycles, which are very close to each other near the single-mode steady state $I_1=I_3=0$, $I_2>0$. Moreover, even for jumps from the cycles lying in the planes Σ_{011} and Σ_{110} to the cycle in the plane Σ_{+1+}, its projection on the plane Σ_{+1+} still remains almost on the unstable cycle lying in the planes Σ_{011} (Σ_{110}) (see Fig. 8).

The chaos associated with dynamical independence is closely related to the symmetry properties of Eqs. (1) and

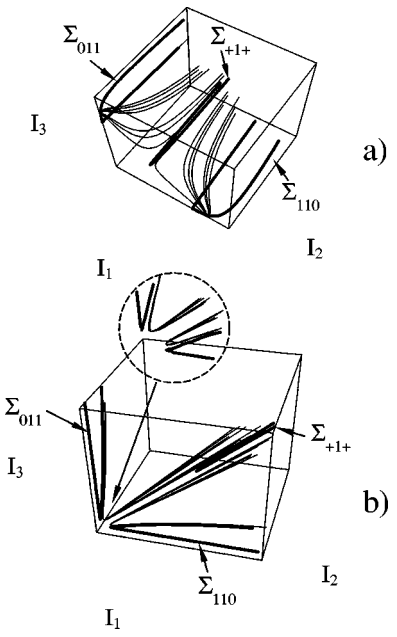

FIG. 7. Enlarged parts of Fig. 6(a) demonstrating jumps between invariant planes. (a) Jumps from Σ_{+1+} to Σ_{011} and Σ_{110}. (b) Jumps from Σ_{011} and Σ_{110} to Σ_{+1+}. Unstable limit cycles in the planes Σ_{011}, Σ_{110}, and Σ_{+1+} are drawn with a bold line.

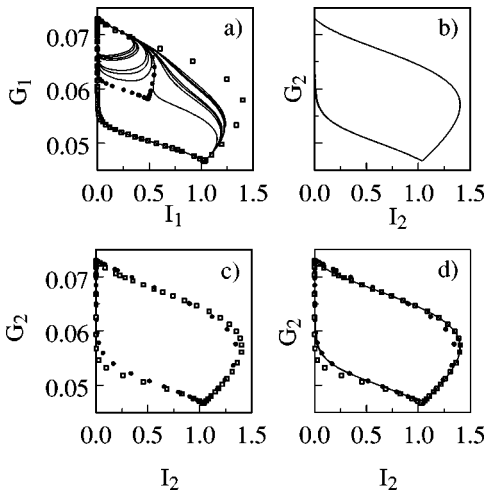

FIG. 8. 2D phase portraits illustrating dynamical independence, shown in Figs. 5 and 6(a). (a) Projection of the chaotic phase trajectory and the unstable limit cycles on the (I_1,G_1) plane. The projection of the unstable cycle lying in the hyperplane Σ_{+1+} (Σ_{110}) is labeled by circles (squares). (b) The same trajectory projected on the (I_2,G_2) plane. (c) The projection of the unstable cycle(s) lying in the hyperplane Σ_{+1+} (Σ_{011} and Σ_{110}) is labeled by circles (squares). (d) Superposition of (b) and (c).

(2). It is worth to stress again that the system retains its symmetry between modes 1 and 3 even for $g \neq 0.5$. This symmetry explains that the cascades of bifurcations for Eqs. (1) and (2) are similar to those described in [16] and [15]. Let us analyze the behavior of the system when varying g. The fixed parameters are the same as for Fig. 4. If $g > 0.5$ is not too large, the limit cycle presented in Fig. 4(b) still remains symmetric but only with respect to the invariant plane Σ_{+1+} [see Fig. 9(a)]. The period of this symmetric stable cycle is twice the period of the two-mode unstable cycles in the hyperplanes Σ_{011} and Σ_{110}. The symmetric cycle loses stability to a pair of asymmetric cycles after a symmetry breaking bifurcation, as shown in Fig. 9(b). This pair of asymmetric cycles becomes a single (possibly homoclinic) orbit and therefore a symmetric cycle occurs by attaching the symmetric pair together. The symmetric cycle is shown in Fig. 9(c). After that, a succession of similar bifurcations takes place, which is illustrated by Figs. 9(b)–9(e). They affect only the behavior of the modes with the same polarization and take place near the invariant planes Σ_{+1+} and Σ_{101}.

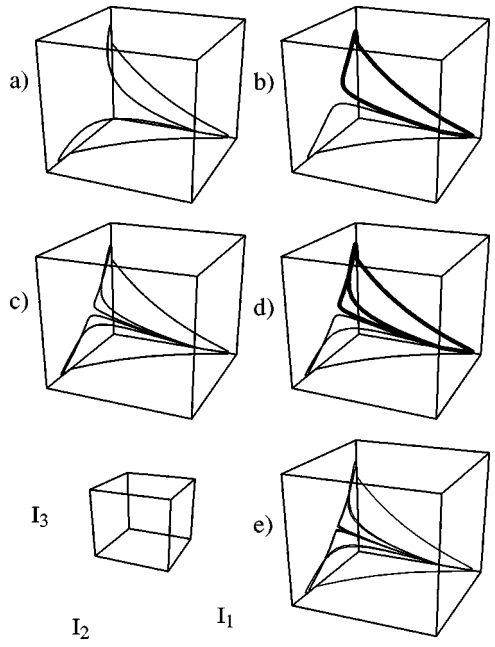

FIG. 9. 3D phase portraits for Eqs. (1) and (2). (a) $g=0.513$, (b) $g=0.5145$, (c) $g=0.515$, (d) $g=0.515\,86$, and (e) $g=0.516$. Other parameters are the same as for Fig. 2. Thin and thick lines correspond to the two asymmetric cycles.

The motion near the invariant planes Σ_{011} and Σ_{110} and, therefore, the behavior of the mode 2, remains almost unaffected. Finally, the sequence produces two asymmetric chaotic attractors which coalesce to form a symmetric attractor. This explains the dynamical independence in the presence of chaos, as mode 2 remains unaffected in the invariant planes Σ_{011} and Σ_{110}, while modes 1 and 3 exhibit chaos near the invariant planes Σ_{+1+} and Σ_{101}.

IV. INFLUENCE OF NOISE

It was shown in [9] that noise added to the system (1) and (2) does not qualitatively affect the dynamically independent mode. Let us consider first what happens with the mechanism of dynamical independence described in the previous section, when a small amplitude constant field is injected into the system and particularly to mode 1 ($\sigma_1 > 0$, $\sigma_{2,3} = 0$). The existence of the invariant plane Σ_{+1+}, characterized by in-phase oscillations for modes within each polarization, results from the symmetry between modes 1 and 3. Injection in one mode only breaks this symmetry and therefore destroys the invariant plane Σ_{+1+}. As a result, the pair of symmetric attractors (one with modes 1,3 and 2, the other with modes 3,1 and 2) no longer exists and the phase trajectory switches to a stable asymmetric limit cycle shown in Fig. 10(a).

Numerical simulations with noise injected in the three-mode regime $\{I_1 = I_3, I_2 > 0\}$ show that the asymmetric cycle is stable if the amplitude of the injection is greater than 10^{-9}. However, the three modes have different responses to the change of the injected amplitude. The motion of mode I_2 remains very close to the unstable cycle lying in the invariant hyperplane Σ_{011} (Σ_{110}) and hardly changes [see Fig. 10(b)], while the amplitudes of oscillations of the modes I_1 and I_3 in the orthogonal polarization change significantly, as shown in Fig. 10(c) for I_3. If the noise is modeled as a random injection [$\sigma_i = \delta\xi_i(t)$, where $\xi_i(t)$, $i=1,2,3$, is a uniform distribution of random numbers on the interval [0,1] and δ is an appropriate amplitude], one could expect that the phase trajectory will always go along the stable cycles corresponding to the different amplitudes of the injection. Therefore, the pair of modes in the same polarization will have noisy oscillations defined by jumps between the stable cycles with different amplitudes, while the mode in the orthogonal polarization will remain unaffected in the invariant hyperplanes Σ_{011} and Σ_{110}.

V. CLUSTERING, GROUPING, AND INDUCED SWITCHING

The other nonreciprocal behaviors previously reported in [10] for $N > 3$ have a similar nature, but the number of in-

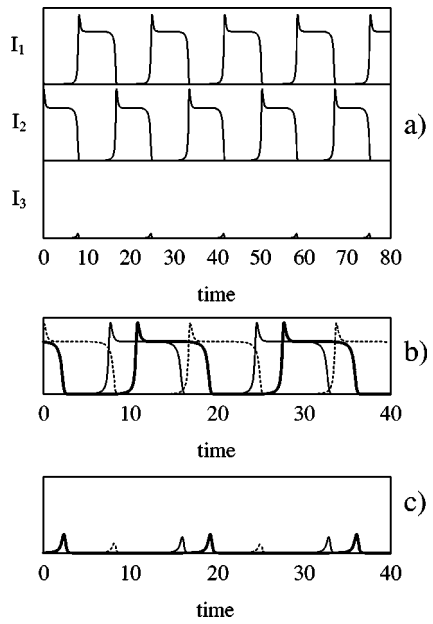

FIG. 10. Three-mode laser subjected to a small amplitude injection σ_1 in mode 1. Modes 1 and 3 have the same polarization and mode 2 is in the orthogonal polarization. Fixed parameters as in Figs. 3. (a) Modal time traces indicate stable periodic behavior for all modes for $\sigma_1=2\times10^{-8}$; (b) time traces of mode 2 for $\sigma_1=2\times10^{-9}$ (bold line), $\sigma_1=4\times10^{-9}$ (thin line), $\sigma_1=10^{-8}$ (dashed line); (c) time traces of mode 3 for $\sigma_1=2\times10^{-9}$ (bold line), $\sigma_1=4\times10^{-9}$ (thin line), $\sigma_1=10^{-8}$ (dashed line).

variant planes containing unstable periodic solutions increases with the mode number N. Two groups of orthogonally polarized modes form a number of different sets of invariant hyperplanes and jumps between them are responsible for grouping, clustering, and self-induced switching. The results of numerical simulations for $N=8$, where six modes are in the same polarization and two modes are in the orthogonal polarization, are shown in Fig. 11. In the clustered state, the six lasing modes with the same polarization emit in-phase pulses while the remaining two modes display antiphase oscillations with equal maxima shifted in such a way that the maxima correspond to minima in the orthogonal polarization. The motion takes place in the invariant subspace defined by equal intensities of the six modes having

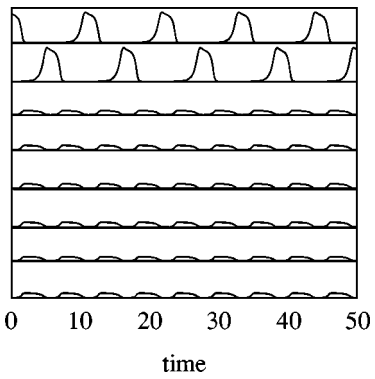

FIG. 11. Clustered state: $N=8$, $\eta=0.002$, $\varepsilon=0.04$, $\alpha=0.02$, $\beta=0.292$, $\gamma=0.11$, $g=0.505$.

the same polarizations and can again be described as a sequential itinerancy in the two invariant planes belonging to this subspace. These planes are similar to the planes Σ_{110} and Σ_{011} of the previous sections.

The motion near a particular invariant plane is almost independent of the remaining phase space, but can define which plane will be the next destination of the phase trajectory. This independence can be used to arrange a switching between different antiphase states. The seeding procedure described in [10] is simply a way to perturb the motion near the plane. There is an unstable antiphase limit cycle lying in an invariant plane and stable within this plane as described in Sec. II and Sec. III. When the phase trajectory moving near this cycle comes close to a single-mode steady-state solution, even a very small perturbation can put it into the vicinity of an unstable cycle lying within another invariant plane. Therefore, if the seeding pulse is chosen appropriately, there will be a switching to a certain antiphase state. An inappropriate choice for timing of a perturbation or pulse intensity can cause a random jump to another hyperplane, and the pattern formation can no longer be predicted.

ACKNOWLEDGMENTS

This research has been supported by the Fonds National de la Recherche Scientifique, the Inter-University Attraction Pole program of the Belgian government, and an INTAS grant.

[1] A. G. Vladimirov, E. A. Viktorov, and P. Mandel, Phys. Rev. E **60**, 1616 (1999).
[2] P. Mandel, *Theoretical Problems in Cavity Nonlinear Optics* (Cambridge University Press, Cambridge, England, 1997).
[3] T. Baer, J. Opt. Soc. Am. B **3**, 1175 (1986).
[4] K. Wiesenfeld, C. Bracikowski, G. James, and R. Roy, Phys. Rev. Lett. **65**, 1749 (1990).
[5] L. Friob, P. Mandel, and E. A. Viktorov, Quantum Semiclassic. Opt. **10**, 1 (1998).
[6] J.-Y. Wang and P. Mandel, Phys. Rev. A **48**, 671 (1993).
[7] A. G. Vladimirov and P. Mandel, Phys. Rev. A **58**, 3320 (1998).
[8] A. G. Vladimirov, Opt. Commun. **149**, 67 (1998).
[9] J.-Y. Wang and P. Mandel, Opt. Lett. **19**, 533 (1994).
[10] K. Otsuka, P. Mandel, and J.-Y. Wang, Opt. Commun. **112**, 71 (1994).
[11] K. Otsuka, Y. Sato, and J.-L. Chern, Phys. Rev. E **56**, 4765 (1997).
[12] E. A. Viktorov and P. Mandel, Quantum Semiclassic. Opt. **8**, 1205 (1996).
[13] E. A. Viktorov and P. Mandel, Opt. Lett. **22**, 1568 (1997).
[14] V. I. Arnold, *Geometrical Methods in the Theory of Ordinary Differential Equations* (Springer, Heidelberg, 1983).
[15] A. Arneodo, P. Coullet, and C. Tresser, Phys. Lett. **81A**, 197 (1981).
[16] P. Glendinning, *Stability, Instability and Chaos* (Cambridge University Press, Cambridge, England, 1994).